Received: 21 October 2019 | Revised: 18 February 2020 | Accepted: 2 March 2020

DOI: 10.1002/alz.12097

Alzheimer's & Dementia®
THE JOURNAL OF THE ALZHEIMER'S ASSOCIATION

FEATURED ARTICLE

In vivo measurement of widespread synaptic loss in Alzheimer's disease with SV2A PET

Adam P. Mecca[1,2] | Ming-Kai Chen[3,5] | Ryan S. O'Dell[1,2] | Mika Naganawa[3] | Takuya Toyonaga[3] | Tyler A. Godek[1,2] | Joanna E. Harris[1,2] | Hugh H. Bartlett[1,2] | Wenzhen Zhao[1,2] | Nabeel B. Nabulsi[3] | Brent C. Vander Wyk[4] | Pradeep Varma[3] | Amy F. T. Arnsten[5] | Yiyun Huang[3] | Richard E. Carson[3] | Christopher H. van Dyck[1,2,5,6]

[1]Alzheimer's Disease Research Unit, Yale University School of Medicine, New Haven, Connecticut

[2]Department of Psychiatry, Yale University School of Medicine, New Haven, Connecticut

[3]Department of Radiology and Biomedical Imaging, Yale University School of Medicine, New Haven, Connecticut

[4]Program on Aging, Yale University School of Medicine, New Haven, Connecticut

[5]Department of Neuroscience, Yale University School of Medicine, New Haven, Connecticut

[6]Department of Neurology, Yale University School of Medicine, New Haven, Connecticut

Correspondence
Adam P. Mecca, Alzheimer's Disease Research Unit, Yale University School of Medicine, One Church Street, 8th Floor, New Haven, CT 06510, USA.
Email: adam.mecca@yale.edu

Funding information
National Institute on Aging, Grant/Award Numbers: P50AG047270, K23AG057784, R01AG052560, R01AG062276, RF1AG057553; American Brain Foundation; Dana Foundation; CTSA, Grant/Award Number: UL1 TR000142; National Center for Advancing Translational Sciences; National Institutes of Health

Abstract

Introduction: Synaptic loss is a robust and consistent pathology in Alzheimer's disease (AD) and the major structural correlate of cognitive impairment. Positron emission tomography (PET) imaging of synaptic vesicle glycoprotein 2A (SV2A) has emerged as a promising biomarker of synaptic density.

Methods: We measured SV2A binding in 34 participants with early AD and 19 cognitively normal (CN) participants using [^{11}C]UCB-J PET and a cerebellar reference region for calculation of the distribution volume ratio.

Results: We observed widespread reductions of SV2A binding in medial temporal and neocortical brain regions in early AD compared to CN participants. These reductions were largely maintained after correction for volume loss and were more extensive than decreases in gray matter volume.

Conclusion: We were able to measure widespread synaptic loss due to AD using [^{11}C]UCB-J PET. Future studies will continue to evaluate the utility of SV2A PET for tracking AD progression and for monitoring potential therapies.

KEYWORDS
[^{11}C]UCB-J | PET, Alzheimer's disease, SV2A, synaptic density

1 | INTRODUCTION

Synaptic loss is an early and robust pathology in Alzheimer's disease (AD)[1,2] and the major structural correlate of cognitive impairment.[3-6] Postmortem and brain biopsy studies have reported lower synapse numbers in hippocampus, frontal cortex, cingulate gyrus, entorhinal cortex, and temporal cortex in AD compared to control participants.[7] Most of these studies have necessarily been conducted in patients with advanced dementia. However, some postmortem work[8-13] has been performed at the prodromal or mild AD stages. These studies have

disproportionately focused on hippocampus as the site of the earliest and most profound synaptic loss,[8-10] consistent with the early degeneration of entorhinal cortical cells projecting via the perforant path to the hippocampus.[14,15] Some pathologic studies of early AD have examined association cortical regions[8,11-13] and have yielded mixed results with regard to synaptic reductions.

With the recent advent of synaptic positron emission tomography (PET) imaging, we have begun to evaluate synaptic alterations in vivo. Synaptic vesicle glycoprotein 2A (SV2A) is expressed in virtually all synapses and is located in synaptic vesicles at presynaptic terminals[16,17] with a conserved expression pattern of about five copies of SV2A per vesicle.[18] [^{11}C]UCB-J was recently developed as a PET tracer for SV2A and advanced for human studies.[19-21] In our initial study of [^{11}C]UCB-J PET in early AD,[22] we reported reduced hippocampal SV2A binding in AD compared with cognitively normal (CN) participants. A recent study using a different SV2A ligand, [^{18}F]UCB-H, also reported reduced synaptic density in AD with the most prominent changes in the hippocampus;[36] however, [^{18}F]UCB-H has been found to have less ideal in vivo imaging properties compared to [^{11}C]UCB-J, including lower specific signal and in vivo affinity for SV2A.[23]

Our preliminary study in early AD with [^{11}C]UCB-J[22] left unclear the regional extent of synaptic alterations that could be demonstrated with this methodology. It also did not address the optimal reference region for SV2A studies of AD. Although the white matter (WM) of the centrum semiovale (CS) has the lowest SV2A specific binding and thus best fulfills the requirement for computing a binding potential (BP_{ND}), it may show too much variance for practical utility in AD. In the present study, we analyzed a substantially larger sample of participants across a somewhat broader range of disease and also re-examined the choice of reference region. We then compared SV2A binding between CN and AD participants across a broader range of brain regions. We also continued to evaluate the relationship between gray matter (GM) tissue loss and SV2A reductions in AD through partial volume correction (PVC) and analysis of volumetric magnetic resonance imaging (MRI) reductions in AD.

RESEARCH IN CONTEXT

1. **Systematic review**: *Postmortem* studies of Alzheimer's disease (AD) have revealed widespread synaptic loss. With the recent advent of synaptic positron emission tomography (PET) imaging, we have begun to evaluate synaptic alterations in vivo. In our initial study of [^{11}C]UCB-J PET in early AD we observed reduced synaptic vesicle glycoprotein 2A (SV2A) binding restricted to the medial temporal lobe.
2. **Interpretation**: In 34 early AD compared to 19 cognitively normal participants, the [^{11}C]UCB-J distribution volume ratio with cerebellum as reference region revealed widespread reductions of SV2A binding in medial temporal and neocortical brain regions. These reductions were largely maintained after correction for volume loss and were more extensive than decreases in gray matter volume.
3. **Future directions**: Further study is needed to define the temporal course of synaptic alterations in AD. Quantification of [^{11}C]UCB-J binding to SV2A in AD may expand our understanding of AD pathogenesis and serve as a novel biomarker for diagnosis and therapeutic efficacy.

2 | METHODS

Detailed methods are described in the Supplementary Material.

2.1 | Study participants and design

Participants aged 55 to 85 years underwent a screening diagnostic evaluation to ensure eligibility. Individuals with AD dementia were required to meet diagnostic criteria for probable dementia due to AD,[24] have a Clinical Dementia Rating (CDR) score of 0.5 to 1.0, and a Mini-Mental Status Examination (MMSE) score <26. Participants with mild cognitive impairment (MCI) were included if they met diagnostic criteria for amnestic MCI,[25] have a CDR score of 0.5, and a MMSE score of 24 to 30, inclusive. Participants with AD dementia and MCI were included if they had impaired episodic memory as evidenced by a Logical Memory II (LMII) score 1.5 standard deviations (SD) below an education-adjusted norm. CN participants were required to have a CDR score of 0, a MMSE score >26, and a normal education-adjusted LMII score. The Rey Auditory Verbal Learning Test (RAVLT) was also administered to generate an episodic memory score. All participants received a PET scan with [^{11}C]Pittsburgh Compound B ([^{11}C]PiB) to determine the presence of brain amyloid β (Aβ) accumulation, as described previously.[22] [^{11}C]PiB PET scans were required to be negative for CN participants and positive for MCI/dementia due to AD participants (Supplementary Methods). All participants provided written informed consent as approved by the Yale University Human Investigation Committee prior to participating in the study.

2.2 | Brain imaging

T1-weighted magnetic resonance imaging (MRI) was performed to define regions of interest (ROIs), and to perform PVC using the Muller-Gartner approach.[22] PET scans were performed on the high-resolution research tomograph (207 slices, resolution <3 mm full with at half maximum (FWHM)[26] with event-by-event motion correction.[27] Dynamic [^{11}C]PiB scans were acquired for 90 minutes following administration of a bolus of up to 555 MBq of tracer.[28] Dynamic [^{11}C]UCB-J scans were acquired for 60 minutes after administration of a bolus of up to 740 MBq.[21] Dynamic PET images were motion corrected (FSL-FLIRT) registered to the participant's MRI.

TABLE 1 Participant characteristics and clinical assessments

	Cognitively normal (A$\beta-$)	Alzheimer's disease (A$\beta+$)	*P*
Participants (*n*)	19	34 (mild dementia: 20, MCI: 14)	
Sex (M/F)	9/10	17/17	0.78
Age (years)	71.7 (8.2) (59-83)	70.2 (7.9) (50-84)	0.50
Education (years)	17.4 (2.1) (12-20)	16.5 (2.5) (12-20)	0.21
CDR-global	0 (0)	0.8 (0.3) (0.5-1.0)	< 0.00001
CDR-SB	0 (0)	4.1 (2.0) (0.5-9.0)	< 0.00001
MMSE	29.3 (1.1) (27-30)	23.1 (4.0) (14-30)	<0.00001
LMII	13.2 (4.3) (5-19)	1.9 (2.5) (0-8)	<0.00001
RAVLT-delay	10.6 (3.2) (4-15)	1.3 (2.1) (0-7)	<0.00001

Data are mean (SD) (range). *P* values are for an unpaired *t* test (continuous variables) or χ^2 test (categorical variables).
CDR-global, clinical dementia rating global score; CDR-SB, clinical dementia rating sum of boxes; LMII, logical memory II score; MMSE, Mini-Mental State Exam; RAVLT, Rey Auditory Verbal Learning Test.

Cortical reconstruction and volumetric segmentation was performed using FreeSurfer [version 6.0].[29] See Tables S1 and S2 for a list of ROIs.

2.3 | Tracer kinetic modeling

For [^{11}C]UCB-J, we first evaluated the suitability of cerebellum (Cb) and CS as reference regions in the subset of participants (12 CN, 18 AD) with arterial blood sampling. We performed kinetic analysis using the 1 tissue compartment (1TC) model to generate parametric images of the volume of distribution V_T.[19,20] We compared V_T between groups for Cb and CS. We then generated parametric images of BP_{ND} for the full participant sample using simplified reference tissue model–2 step (SRTM2)[30] and a small ROI (2 mL) in the core of the CS as reference region[31,32] and also calculated the distribution volume ratio (*DVR*) with a CS reference region (DVR_{CS}) = BP_{ND}+1. The use of SRTM2 requires a global k'$_2$ value (clearance rate constant, k_2, of the reference region), which was computed as a population average of k_2 of the CS obtained using the 1TC model (k'$_2$ = 0.027 min^{-1}; from a previous group of subjects with arterial blood sampling). Finally, DVR_{Cb} of each voxel was computed from DVR_{CS} as (BP_{ND} +1)/(BP_{ND}[cerebellum]+1). For whole cortex (vertex-wise) analysis, parametric PET images were sampled to the cortical surface in subject-space and spatially smoothed using a 10 mm FWHM gaussian kernel prior to statistical analysis.

2.4 | Statistical analyses

Statistical methods are detailed in the supplementary materials. Briefly, χ^2 tests were used for group comparisons of categorical variables and unpaired *t* tests for continuous variables. Linear mixed models were used to compare SV2A *DVR* or brain volume between AD and CN groups. Post hoc comparisons utilized unpaired *t* tests. For the primary analyses of DVR_{Cb}, the Benjamini-Hochberg procedure was used to control the false discovery rate for multiple comparisons. Other analyses were treated as exploratory, and no multiplicity corrections were applied. For display, effect size (Cohen's d) maps were created by producing images with the voxels in each FreeSurfer region set uniformly to the calculated effect size for that region. Pearson's correlation was used to assess relationships between *DVR* and episodic memory or global function. Tests were two-tailed and used $P < 0.05$ as a threshold for significance.

3 | RESULTS

3.1 | Participant characteristics

The study sample consisted of 53 participants—34 with amnestic MCI due to AD or mild AD dementia and 19 who were CN. Diagnostic groups were well balanced for age, sex, and education (Table 1). AD participants had clinical characteristics typical of amnestic MCI and mild AD dementia with MMSE = 23.1(mean) ± 4.1 (SD) and CDR = 0.74 ± 0.25.

3.2 | Investigation and validation of reference regions

In the subset of participants (12 CN, 18 AD) with arterial blood sampling, the distribution volume V_T was very similar between groups for either Cb (AD: 13.06 ± 1.69, CN: 13.22 ± 1.54, unpaired *t* test, P = 0.80) or CS (AD: 4.00 ± 0.63, CN: 4.10 ± 0.38, unpaired *t* test, P = 0.63), supporting the validity of both reference regions. Moreover, values of DVR_{Cb} converted from DVR_{CS} (obtained from SRTM2) were highly correlated with values of DVR_{Cb} obtained with the 1TC model across all brain regions (Figure S1). Finally, values of DVR_{Cb} compared to DVR_{CS} showed significantly lower coefficients of variation (CoVs) across brain regions of interest for both the 1TC subsample (data not shown) and the full sample (modified signed-likelihood ratio test, $P < 0.05$) (Table S3). Therefore, in our primary investigation of group differences in SV2A binding, we focused on DVR_{Cb} but also analyzed BP_{ND} with CS as reference region for comparison with previous results.

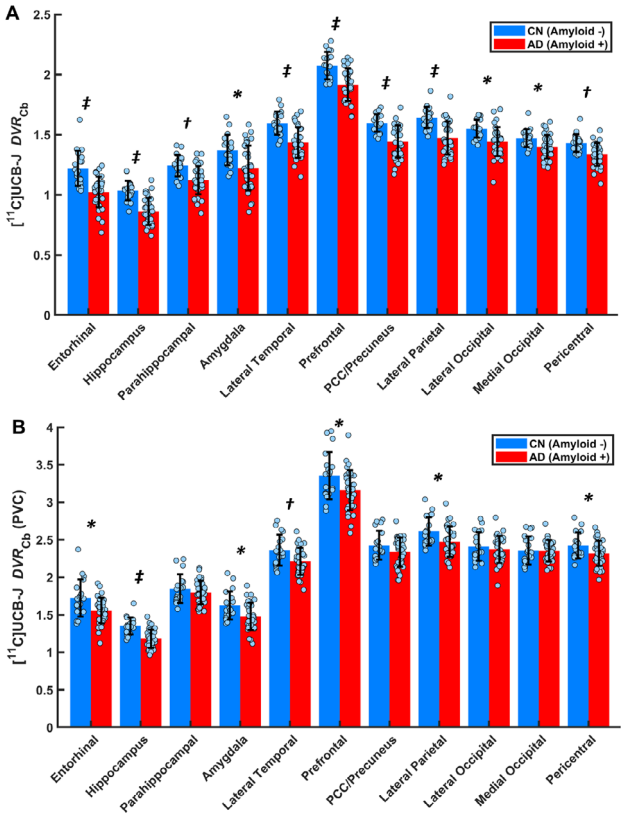

FIGURE 1 Comparison of synaptic density in AD and CN groups using DVR_{Cb} (A) before and (B) after partial volume correction (PVC). $^{*}P < 0.05$, $^{\dagger}P < 0.001$, $^{\ddagger}P < 0.0001$ for post hoc *t* tests comparing AD ($n = 19$) and CN ($n = 34$) groups. False discovery rate correction for multiple comparisons is shown in Table 2. Dots represent the DVR_{Cb} for each participant. Error bars represent standard deviations. Abbreviations: DVR_{Cb}, distribution volume ratio using a cerebellum reference region; CN, cognitively normal, AD, Alzheimer's disease.

3.3 | Synaptic density in AD compared to CN participants

The primary analysis of DVR_{Cb} demonstrated a significant effect of group ($F(1,51) = 33.4$, $P < 0.00001$) and group*region ($F(10,510) = 2.4$, $P = 0.01$) as predictors of SV2A binding (DVR_{Cb}). Post hoc comparisons revealed significant SV2A reductions in AD compared to CN participants in all medial temporal regions, as well as more broadly in neocortical regions (Figure 1A, Table 2). Group differences were most pronounced in the hippocampus and entorhinal cortex but were also present in the parahippocampal cortex, amygdala, lateral temporal cortex, prefrontal cortex, posterior cingulate cortex (PCC)/precuneus, lateral parietal cortex, and pericentral cortex. Average group images of DVR_{Cb} were consistent with SV2A availability throughout the neocortex and medial temporal lobe structures but with visibly reduced [11C]UCB-J binding in AD in many regions (Figure 2). When the AD group was separated into MCI and dementia subgroups, similar results were observed (Figure S2A, Table S4A). Finally, additional models that included covariates of age, sex, and education did not alter the results.

The secondary analysis of BP_{ND} using CS as the reference region showed no significant effect of group ($F(1,51) = 2.1$, $P = 0.16$), but a significant interaction of group*region ($F(10,510) = 2.0$, $P = 0.04$). Post hoc comparisons revealed group differences that were significant only in the hippocampus and entorhinal cortex (Table 3, Figure S3). Hippocampal BP_{ND} was 20% lower in the AD group compared to the CN group. To permit direct comparison of our current results (using FreeSurfer ROIs) to our previous results (using automated anatomical labeling ROIs), we evaluated separately the 21 participants who were also included in our previous report.[22] In that subsample, hippocampal BP_{ND} was 25% lower in AD (n = 10) compared to CN (n = 11) participants using FreeSurfer ROIs (See Discussion 4.1.).

TABLE 2 SV2A ([11C]UCB-J DVR_{Cb}) in regions of interest—cerebellum reference region

	DVR_{Cb}			DVR_{Cb}—partial volume corrected		
Region	CN ($n = 19$) Mean (SD)	AD ($n = 34$) Mean (SD)	*P*	CN ($n = 19$) Mean (SD)	AD ($n = 34$) Mean (SD)	*P*
Entorhinal	1.21 (0.15)	1.02 (0.13)	<0.00001*,†	1.72 (0.25)	1.56 (0.17)	0.005*,†
Hippocampus	1.04 (0.08)	0.86 (0.11)	<0.00001*,†	1.35 (0.11)	1.18 (0.12)	<0.00001*,†
Parahippocampal	1.24 (0.09)	1.12 (0.12)	0.0003*,†	1.85 (0.19)	1.80 (0.16)	0.32
Amygdala	1.37 (0.13)	1.22 (0.19)	0.003*,†	1.62 (0.19)	1.48 (0.18)	0.009*,†
Lateral temporal	1.60 (0.09)	1.43 (0.13)	<0.0001*,†	2.36 (0.21)	2.21 (0.18)	0.009*,†
Prefrontal	2.07 (0.11)	1.92 (0.14)	<0.0001*,†	3.35 (0.31)	3.16 (0.27)	0.02*,†
PCC/Precuneus	1.60 (0.07)	1.44 (0.13)	<0.0001*,†	2.43 (0.19)	2.34 (0.20)	0.11
Lateral parietal	1.64 (0.09)	1.47 (0.13)	<0.0001*,†	2.61 (0.19)	2.47 (0.20)	0.02*,†
Lateral occipital	1.55 (0.08)	1.44 (0.12)	0.001*,†	2.41 (0.19)	2.37 (0.18)	0.47
Medial occipital	1.47 (0.07)	1.40 (0.10)	0.008*,†	2.36 (0.19)	2.35 (0.14)	0.95
Pericentral	1.43 (0.07)	1.34 (0.09)	0.0005*,†	2.43 (0.17)	2.32 (0.17)	0.03*

Data are mean (SD). *P*-values are for post hoc two-tailed, unpaired *t* tests (uncorrected for multiplicity) performed after a linear mixed model analysis of *DVR* in multiple regions (within-subject factor) between CN and AD diagnostic groups.

AD, Alzheimer's disease; CN, cognitively normal; DVR_{Cb}, distribution volume ratio of [11C]UCB-J in regions of interest calculated with a cerebellum reference region.

*$P < 0.05$ prior to false discovery rate correction for multiple comparisons.

†$P < 0.05$ after false discovery rate correction.

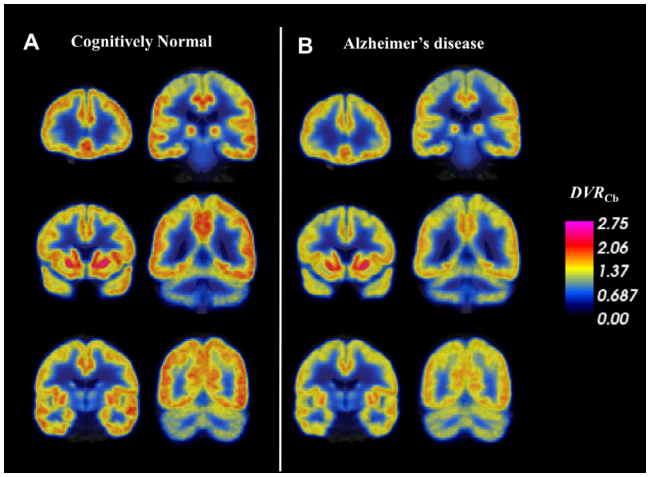

FIGURE 2 Synaptic density (DVR_{Cb}) in AD and CN groups determined by [^{11}C]UCB-J PET. Coronal sections of average parametric images of DVR_{Cb} for (A) 19 CN participants and (B) 34 AD participants. Average images are created after co-registration to a common MNI template. The average parametric PET scans are displayed in pseudo-color representing [^{11}C]UCB-J binding to SV2A (DVR_{Cb}) and overlaid on the MNI template T1 MRI. Lower DVR_{Cb} in AD compared to CN participants was apparent in the medial temporal lobe and throughout the cortex and subcortex.

3.4 | Corrections for partial volume effects

To evaluate the contribution of partial volume effects to SV2A reductions in AD, we repeated the previous analyses following PVC. The primary analysis of DVR_{Cb} again demonstrated a significant effect of group ($F(1,51) = 7.7$, $P = 0.008$) and group*region ($F(10,510) = 3.1$, $P = 0.001$) on DVR_{Cb}. Post hoc comparisons revealed continued significant SV2A reduction in the hippocampus, entorhinal cortex, amygdala, lateral temporal cortex, prefrontal cortex, lateral parietal cortex, and pericentral cortex, but not in the parahippocampal cortex, PCC/precuneus, lateral occipital cortex, or medial occipital cortex (Figure 1B, Table 2). When the AD group was separated into MCI and dementia subgroups, similar results were observed (Figure S2B, Table S4B).

The corresponding PVC analyses of BP_{ND} using CS as the reference region showed no significant effect of group ($F(1,51) = 0.2$, $P = 0.70$, but a significant interaction of group*region ($F(10,510) = 0.2$, $P = 0.004$). Post hoc comparisons revealed only a significant group difference in the hippocampus (Table 3).

To compare the patterns of synaptic loss and volume loss in AD, we performed a volumetric MRI analysis to assess GM volume differences between AD and CN groups. Linear mixed model analysis, including group, region, and the group*region interaction as predictors, demonstrated a significant effect of group ($F(1,51) = 16.0$, $P = 0.00009$) and group*region ($F(10,510) = 2.4$, $P = 0.01$) on GM volume. We observed a significant volume reduction in the hippocampus, entorhinal cortex, parahippocampal cortex, amygdala, lateral temporal cortex, PCC/precuneus, and lateral parietal cortex, but not in the prefrontal cortex, lateral occipital cortex, medial occipital cortex, or pericentral cortex (Figure S4, Table S5).

3.5 | Whole brain analyses

Exploratory whole brain analyses were performed on both a regional (all FreeSurfer Desikan-Killiany regions) and whole cortex (vertex-wise) level. For all FreeSurfer regions, the effect size (Cohen's d) for group difference was calculated for DVR_{Cb} with and without PVC, as well as for brain volume (Figure 3). Consistent with the primary regional analyses, the largest effect sizes for DVR_{Cb} were found in the hippocampus, but also in a wide range of cortical and

TABLE 3 SV2A ([^{11}C]UCB-J BP_{ND}) in regions of interest—centrum semiovale reference region

	BP_{ND}			BP_{ND}—partial volume corrected		
Region	CN ($n = 19$) Mean (SD)	AD ($n = 34$) Mean (SD)	P	CN ($n = 19$) Mean (SD)	AD ($n = 34$) Mean (SD)	P
Entorhinal	3.07 (0.71)	2.53 (0.63)	0.006*	4.75 (1.07)	4.37 (0.91)	0.18
Hippocampus	2.47 (0.61)	1.98 (0.60)	0.006*	3.52 (0.72)	3.09 (0.74)	0.049*
Parahippocampal	3.16 (0.69)	2.88 (0.72)	0.18	5.18 (1.09)	5.21 (1.01)	0.90
Amygdala	3.58 (0.79)	3.21 (0.83)	0.12	4.41 (0.84)	4.10 (0.89)	0.22
Lateral temporal	4.34 (0.90)	3.97 (0.90)	0.15	6.88 (1.14)	6.65 (1.26)	0.53
Prefrontal	7.63 (1.18)	5.31 (1.07)	0.32	9.85 (1.47)	9.60 (1.68)	0.59
PCC/Precuneus	4.36 (1.01)	4.00 (0.89)	0.18	7.10 (1.20)	7.08 (1.35)	0.98
Lateral parietal	4.52 (1.09)	4.11 (0.95)	0.15	7.73 (1.36)	7.57 (1.46)	0.68
Lateral occipital	4.21 (0.99)	4.01 (0.95)	0.47	7.05 (1.26)	7.22 (1.43)	0.68
Medial occipital	3.93 (0.86)	3.84 (0.82)	0.71	6.87 (1.17)	7.13 (1.24)	0.45
Pericentral	3.81 (0.95)	3.62 (0.76)	0.42	7.10 (1.21)	7.02 (1.29)	0.81

Data are mean (SD). P-values are for post hoc two-tailed, unpaired t tests (uncorrected for multiplicity) performed after a linear mixed model analysis of BP_{ND} in multiple regions (within-subject factor) between CN and AD diagnostic groups.
AD, Alzheimer's disease; BP_{ND}, binding potential non-displaceable for [^{11}C]UCB-J in regions of interest calculated with a centrum semiovale reference region; CN, cognitively normal.
*$P < 0.05$.

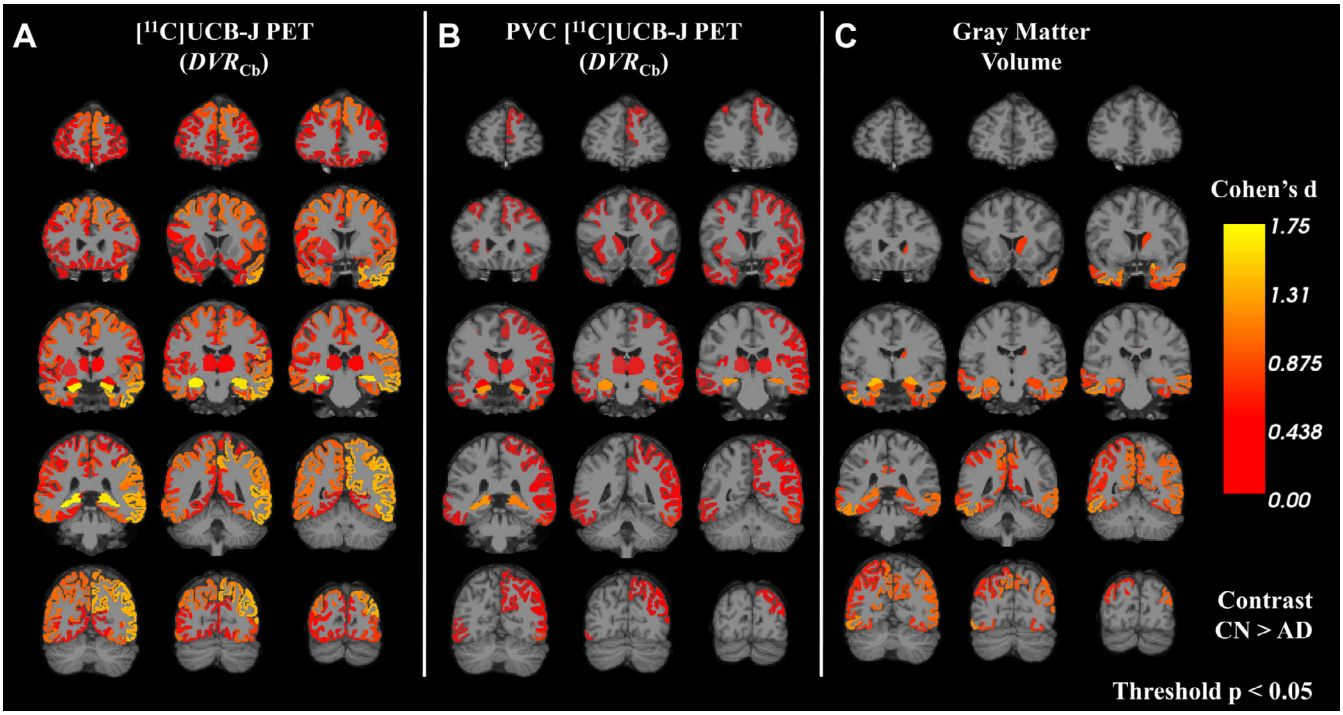

FIGURE 3 Effect-size maps of synaptic density (DVR_{Cb}) and brain volume between AD and CN groups. Effect sizes for differences in AD compared to CN groups were calculated for (A) uncorrected [^{11}C]UCB-J PET, (B) PVC [^{11}C]UCB-J PET, and brain volume (C) in all FreeSurfer regions. The color scale represents Cohen's d for the comparison between CN and AD group. Effect size statistics are displayed only for regions that had an uncorrected $P < 0.05$. Contrast is for CN>AD. Abbreviations: CN, cognitively normal; AD, Alzheimer's disease; PET, positron emission tomography; DVR_{Cb}, distribution volume ratio using a cerebellum reference region.

subcortical regions (Figure 3A). After PVC was applied, this pattern was similar but with reduced effect sizes (Figure 3B). For brain volumes, the pattern remained somewhat similar, but with still smaller effect sizes (Figure 3C). Table S6 presents group differences (unpaired *t* tests) for all ROIs included in Figure 3.

Additional exploratory whole brain analyses used a surface-based approach. Consistent with the multi-region analysis, synaptic density showed widespread neocortical reductions in the AD group, with notable sparing around the central sulcus and primary visual cortex (Figure S5).

3.6 | Association between synaptic density and clinical measures

In an exploratory analysis of the relationship between synaptic density and clinical measures, we investigated the association of hippocampal or composite DVR_{Cb} with CDR sum of boxes (CDR-SB) or episodic memory. In the overall sample, statistically significant correlations were found between hippocampal DVR_{Cb} and CDR-SB ($r = -0.62$, $P < 0.00001$) or episodic memory ($r = 0.67$, $P < 0.00001$) (Figure S6A and S6B). When a composite ROI of AD-affected regions (entorhinal, hippocampus, parahippocampal, amygdala, prefrontal, lateral temporal, PCC/precuneus, lateral parietal, and lateral occipital regions) was used, statistically significant correlations were present between DVR_{Cb} and CDR-SB ($r = -0.54$, $P = 0.00003$) or episodic memory ($r = 0.56$, $P = 0.00001$) (Figure S6C and S6D). None of these correlations were significant within the AD or CN groups.

4 | DISCUSSION

We used [^{11}C]UCB-J PET to investigate SV2A binding in early AD. We first investigated the validity of reference regions (CS vs cerebellum) and found that, although both regions evidenced comparable V_T in AD and CN groups, values of DVR_{Cb} demonstrated significantly lower variability (CoV) than DVR_{CS}, favoring its use in studies of AD. Using DVR_{Cb} as our primary outcome, we observed a broad pattern of reductions in synaptic density in all of the medial temporal and neocortical brain regions analyzed.

When we evaluated the contribution of partial volume effects to SV2A reductions in AD, group differences in regional DVR_{Cb} after PVC, remained significant in most but not all regions. We further explored the relationship between GM atrophy and SV2A reductions using a volumetric MRI analysis, which revealed significant volume reductions in AD in all medial temporal regions, but in a distribution of neocortical regions that was less widespread than for synaptic loss. Additional exploratory analyses suggested that hippocampal synaptic density was associated with episodic memory performance and inversely associated with global function (CDR-SB) in the overall sample.

4.1 | Comparison with previous human synaptic density imaging studies

These results confirm our previous report of reduced hippocampal SV2A binding in AD compared with CN participants using [^{11}C]UCB-J PET[22] but extend them to include significant reductions in other medial temporal and, particularly, in several neocortical brain regions. When comparing the magnitude of reduction in hippocampal binding to that in our earlier report,[22] hippocampal BP_{ND} with CS as reference region was reduced by 20% in the present study, instead of 44% (or 27% with a GM mask applied, which is more similar to the FreeSurfer segmentation process utilized in the present study, minimizing the contribution of GM atrophy). To confirm that the discrepant results were related to a change in ROI methods, we compared data for the participants common to both studies (11 CN, 10 AD) and found that hippocampal BP_{ND} was 25% lower in the AD compared to CN participants in the present study, which is close to the 27% reduction we reported previously with application of a GM mask.[22] Differences in the regional extent of significant SV2A reductions in the present investigation are likely attributable to the larger sample size and somewhat broader range of disease stage, but also—and more substantially—to the difference in reference region for normalization, as discussed below. Indeed, the secondary results of BP_{ND} with CS as reference region are quite similar to our previous results using the same outcome,[22] with significant reductions limited to hippocampus and entorhinal cortex.

Our findings are also consistent with a recent report using [^{18}F]UCB-H PET[33] in which significant reductions of tracer binding to SV2A in AD were initially restricted to the hippocampus, but—unlike in our study—became more widespread after PVC. This difference in the effects of PVC may be due to lower specific-to-nonspecific binding[22] and thus lower image contrast for [^{18}F]UCB-H, which is improved by reduced spillover of estimated activity following PVC.

4.2 | Comparison with postmortem and biopsy specimen human studies

Considerable postmortem and brain biopsy research has been devoted to the characterization of synaptic loss in AD. A recent meta-analysis[7] used 22 references to evaluate the regional extent of synaptic reductions in AD and reported consistently more reductions in hippocampus, frontal cortex, and the combined regions of cingulate gyrus, entorhinal cortex, and temporal cortex. Most postmortem studies—including the majority of the references included in this meta-analysis[7]—have necessarily been conducted in patients with advanced dementia. However, some postmortem work[8-11,13] has been performed in patients at the prodromal or mild AD stages. These studies have disproportionately focused on hippocampus as the site of earliest and most profound synaptic loss, consistent with the early degeneration of entorhinal cortical cells,[14,34] projecting via the perforant path to all fields of the hippocampal formation, including the dentate gyrus, Cornu Ammonis (CA) fields, and the subiculum. Indeed, pathology studies have reported a reduction in synapses in the outer molecular layer of dentate gyrus of 44% in mild AD and 13% to 20% in MCI,[8,9] as well as a reduction of 55% in patients with mild AD and 18% in patients with MCI in the CA1 field.[10] These postmortem findings are consistent with the reductions in SV2A binding observed in the present study, in vivo, with [^{11}C]UCB-J PET, as measured by BP_{ND} with CS as the reference region (20%).

Some,[12,13] but not all,[8,11] pathologic studies of association cortical regions in participants with early AD have shown synaptic reductions. Our results are difficult to compare directly to these limited studies because we employ different ROIs. Consistent with these results, we observed reductions in lateral temporal cortex (which includes the inferior temporal gyrus studied by Scheff et al.[13]) and the PCC/precuneus region (which includes two regions analyzed separately by Scheff et al.).[11,12] Our finding of SV2A reductions in brain regions that incorporate primary sensory and motor cortices cannot be compared to postmortem studies, which have not examined these regions. However, these results are explainable by the vast inputs to these regions from association cortical regions that contain primary AD pathology. For example, the only pure sensorimotor region we examined (pericentral cortex) receives major direct inputs from premotor cortex and cingulate cortex to primary motor cortex[35,36] and from parietal association cortex to primary somatosensory cortex.[37]

4.3 | Validation and limitations of tissue reference regions

We previously validated the measurement of SV2A binding using the white matter of the CS reference region,[20] and also validated the use of a bloodless binding potential (BP_{ND}), specifically in participants with AD.[22] BP_{ND} images obtained with the simplified reference tissue models[30] have given values with excellent agreement to those computed from 1TC V_T maps. BP_{ND} assumes a reference region with negligible specific binding, which has been demonstrated previously with displacement by the SV2A-selective anticonvulsant levetiracetam.[20,38] In the present investigation, we propose that in the setting of AD, cerebellum may also serve as a suitable reference region and may possess practical superiority over CS due to lower intersubject variability. Although cerebellum has considerable SV2A-specific binding and thus is unsuitable for computing the binding potential (BP_{ND}), it demonstrates minimal (~1%) difference between CN and AD participants in V_T from 1TC modeling, suggesting that it may be used in computing *DVR*. As shown in Table 3, the use of CS as reference in the same sample yielded results similar to our original publication, with prominent reductions in hippocampus and entorhinal cortex but not in neocortical regions. This difference in results appears to accrue largely from a significantly smaller CoV for DVR_{Cb} compared to DVR_{CS} (Table S3).

For most studies with [^{11}C]UCB-J, the CS may serve as an optimal reference region in the sense that it best represents nondisplaceable binding and permits calculation of the more quantitative outcome measure that is proportional to B_{max}.[39] However, the reduced sensitivity of the CS for studies in AD may be attributed to significantly greater variability of the CS measure, owing to a smaller ROI and lower activity levels. Moreover, although CS is devoid of presynaptic terminals, it

has been shown to contain a small amount of specific binding.[32] Even when optimized to minimize spill-in through the use of a smaller ROI, CS V_T exceeded the GM non-displaceable binding (V_{ND}) by ~35% to 40%. This specific SV2A binding in the WM of the CS may reflect a number of factors, particularly axonal transport of synaptic vesicles.[32] The white matter tracts of the CS contain many corticocortical association fibers[40] which—like their terminals in the neocortical gray matter—are likely to contain reduced SV2A binding in AD. Therefore, BP_{ND} with CS as reference region may not only underestimate BP_{ND}, but may suffer from a small bias between diagnostic groups, thus underestimating reductions in synaptic density in AD. A similar theoretical limitation of the cerebellum as reference region is that—although it contains minimal intrinsic AD neuropathology—it may receive presynaptic terminals that are altered in AD. Most nerve terminals within cerebellum are from brain regions unaffected by AD,[41] as the input from association cortices is by pontocerebellar relay fibers.[42,43] However, a portion of the projections to cerebellum are directly from locus ceruleus,[44] which contains some of the earliest neurofibrillary tangless in AD.[14] Therefore, DVR_{Cb}, like BP_{ND} with CS as reference region, may tend to underestimate reductions in synaptic density in AD, although we observed no statistically significant group differences in CS or cerebellar V_T values in a subsample of the present cohort.

4.4 | Limitations

This study has a number of limitations. The diagnosis of AD was made on the basis of standard clinical criteria combined with amyloid PET positivity. No assessment was made of biomarkers of tau pathogenesis, or of neuropathology at autopsy. In addition, our study has limited power for investigating the effects of important demographic variables such as age, sex, and education, due to the modest sample size. Future studies of larger samples and a broader range of educational attainment may permit a better understanding of how these variables interact with AD to alter synaptic density.

4.5 | Conclusions and future directions

We observed widespread reductions of synaptic density using [^{11}C]UCB-J PET in medial temporal and neocortical brain regions in early AD compared to CN participants. Most of these reductions were maintained after PVC and thus are not attributable solely to GM tissue loss, which appears to be of lower magnitude and regional extent on structural MRI. Further studies are needed to examine the relationship between synaptic density and other MRI measures, including structural connectivity using diffusion tensor imaging, and functional connectivity using functional MRI. Longitudinal and multi-tracer studies are needed to characterize the temporal course of synaptic alterations in AD in relation to amyloid and tau accumulation, as well as the associations with cognitive and functional change. Quantification of [^{11}C]UCB-J binding to SV2A in AD may expand our understanding of AD pathogenesis and serve as a novel biomarkers for diagnosis and therapeutic efficacy.

ACKNOWLEDGEMENTS

We wish to thank the research participants for their contributions, and the staff of the Yale PET Center for their excellent technical assistance. We also thank UCB for providing the [^{11}C]UCB-J radiolabeling precursor and the unlabeled reference standard. This research was supported by the National Institute on Aging (P50AG047270, K23AG057784, and R01AG052560, R01AG062276, and RF1AG057553), The American Brain Foundation (APM), and The Dana Foundation (MKC). This publication was made possible by CTSA Grant Number UL1 TR000142 from the National Center for Advancing Translational Sciences (NCATS), a component of the National Institutes of Health (NIH). Its contents are solely the responsibility of the authors and do not necessarily represent the official view of NIH.

DECLARATIONS OF INTEREST

Adam P. Mecca, Richard E. Carson, and Christopher H. van Dyck report grants from National Institutes of Health for the conduct of the study. Adam P. Mecca reports grants for clinical trials from Genentech and Eisai outside the submitted work. Ming-Kai Chen reports research support from the Dana Foundation and research support from Eli Lilly and clinical trials from Merck outside the submitted work. Yiyun Huang reports research grants from UCB and Eli Lilly outside the submitted work. Yiyun Huang and Richard E. Carson have a patent for a newer version of the tracer. Richard E. Carson is a consultant for Rodin Therapeutics and has received research funding from UCB. Richard E. Carson reports having received grants from AstraZeneca, Astellas, Eli Lilly, Pfizer, Taisho, and UCB outside the submitted work. Christopher H. van Dyck reports consulting fees from Kyowa Kirin, Roche, Merck, Eli Lilly, and Janssen and grants for clinical trials from Biogen, Novartis, Eli Lilly, Merck, Eisai, Janssen, Roche, Genentech, Toyama, and Biohaven, outside the submitted work. No other disclosures are reported.

REFERENCES

1. Scheff SW, DeKosky ST, Price DA. Quantitative assessment of cortical synaptic density in Alzheimer's disease. *Neurobiol Aging*. 1990;11:29-37.
2. Selkoe DJ. Alzheimer's disease is a synaptic failure. *Science*. 2002;298:789-791.
3. Terry RD, Masliah E, Salmon DP, et al. Physical basis of cognitive alterations in Alzheimer's disease: synapse loss is the major correlate of cognitive impairment. *Ann Neurol*. 1991;30:572-580.
4. DeKosky ST, Scheff SW. Synapse loss in frontal cortex biopsies in Alzheimer's disease: correlation with cognitive severity. *Ann Neurol*. 1990;27:457-464.
5. DeKosky ST, Scheff SW, Styren SD. Structural correlates of cognition in dementia: quantification and assessment of synapse change. *Neurodegeneration*. 1996;5:417-421.
6. Hamos JE, DeGennaro LJ, Drachman DA. Synaptic loss in Alzheimer's disease and other dementias. *Neurology*. 1989;39:355-361.
7. de Wilde MC, Overk CR, Sijben JW, Masliah E. Meta-analysis of synaptic pathology in Alzheimer's disease reveals selective molecular vesicular machinery vulnerability. *Alzheimers Dement*. 2016;12:633-644.

8. Masliah E, Mallory M, Hansen L, DeTeresa R, Alford M, Terry R. Synaptic and neuritic alterations during the progression of Alzheimer's disease. *Neurosci Lett*. 1994;174:67-72.
9. Scheff SW, Price DA, Schmitt FA, Mufson EJ. Hippocampal synaptic loss in early Alzheimer's disease and mild cognitive impairment. *Neurobiol Aging*. 2006;27:1372-1384.
10. Scheff SW, Price DA, Schmitt FA, DeKosky ST, Mufson EJ. Synaptic alterations in CA1 in mild Alzheimer disease and mild cognitive impairment. *Neurology*. 2007;68:1501-1508.
11. Scheff SW, Price DA, Schmitt FA, Roberts KN, Ikonomovic MD, Mufson EJ. Synapse stability in the precuneus early in the progression of Alzheimer's disease. *J Alzheimers Dis*. 2013;35:599-609.
12. Scheff SW, Price DA, Ansari MA, et al. Synaptic change in the posterior cingulate gyrus in the progression of Alzheimer's disease. *J Alzheimers Dis*. 2015;43:1073-1090.
13. Scheff SW, Price DA, Schmitt FA, Scheff MA, Mufson EJ. Synaptic loss in the inferior temporal gyrus in mild cognitive impairment and Alzheimer's disease. *J Alzheimers Dis*. 2011;24:547-557.
14. Braak H, Thal DR, Ghebremedhin E, Del Tredici K. Stages of the pathologic process in Alzheimer disease: age categories from 1 to 100 years. *J Neuropathol Exp Neurol*. 2011;70:960-969.
15. Gomez-Isla T, West HL, Rebeck GW, et al. Clinical and pathological correlates of apolipoprotein E e4 in Alzheimer's disease. *Ann Neurol*. 1996;39:62-70.
16. Bajjalieh SM, Frantz GD, Weimann JM, McConnell SK, Scheller RH. Differential expression of synaptic vesicle protein 2 (SV2) isoforms. *J Neurosci*. 1994;14:5223-5235.
17. Bajjalieh SM, Peterson K, Linial M, Scheller RH. Brain contains two forms of synaptic vesicle protein 2. *Proc Natl Acad Sci U S A*. 1993;90:2150-2154.
18. Mutch SA, Kensel-Hammes P, Gadd JC, et al. Protein quantification at the single vesicle level reveals that a subset of synaptic vesicle proteins are trafficked with high precision. *J Neurosci*. 2011;31:1461-1470.
19. Nabulsi N, Mercier J, Holden D, et al. Synthesis and Preclinical Evaluation of 11C-UCB-J as a PET Tracer for Imaging the Synaptic Vesicle Glycoprotein 2A in the Brain. *J Nucl Med*. 2016;57(5):777-784.
20. Finnema SJ, Nabulsi NB, Eid T, et al. Imaging synaptic density in the living human brain. *Sci Transl Med*. 2016;8:348ra96.
21. Finnema SJ, Nabulsi NB, Mercier J, et al. Kinetic evaluation and test-retest reproducibility of [(11)C]UCB-J, a novel radioligand for positron emission tomography imaging of synaptic vesicle glycoprotein 2A in humans. *J Cereb Blood Flow Metab*. 2018;38:2041-2052.
22. Chen MK, Mecca AP, Naganawa M, et al. Assessing Synaptic Density in Alzheimer Disease With Synaptic Vesicle Glycoprotein 2A Positron Emission Tomographic Imaging. *JAMA Neurol*. 2018;75:1215-24.
23. Constantinescu CC, Tresse C, Zheng M, et al. Development and In Vivo Preclinical Imaging of Fluorine-18-Labeled Synaptic Vesicle Protein 2A (SV2A) PET Tracers. *Mol Imaging Biol*. 2019;21:509-518.
24. McKhann GM, Knopman DS, Chertkow H, et al. The diagnosis of dementia due to Alzheimer's disease: recommendations from the National Institute on Aging-Alzheimer's Association workgroups on diagnostic guidelines for Alzheimer's disease. *Alzheimers Dement*. 2011;7:263-269.
25. Albert MS, DeKosky ST, Dickson D, et al. The diagnosis of mild cognitive impairment due to Alzheimer's disease: recommendations from the National Institute on Aging-Alzheimer's Association workgroups on diagnostic guidelines for Alzheimer's disease. *Alzheimers Dement*. 2011;7:270-279.
26. de Jong HW, van Velden FH, Kloet RW, Buijs FL, Boellaard R, Lammertsma AA. Performance evaluation of the ECAT HRRT: an LSO-LYSO double layer high resolution, high sensitivity scanner. *Phys Med Biol*. 2007;52:1505-1526.
27. Jin X, Mulnix T, Gallezot JD, Carson RE. Evaluation of motion correction methods in human brain PET imaging–a simulation study based on human motion data. *Med Phys*. 2013;40:102503.
28. Mecca AP, Barcelos NM, Wang S, et al. Cortical beta-amyloid burden, gray matter, and memory in adults at varying APOE epsilon4 risk for Alzheimer's disease. *Neurobiol Aging*. 2017;61:207-214.
29. Fischl B. FreeSurfer. *Neuroimage*. 2012;62:774-781.
30. Wu Y, Carson RE. Noise reduction in the simplified reference tissue model for neuroreceptor functional imaging. *J Cereb Blood Flow Metab*. 2002;22:1440-52.
31. Mertens N, Maguire RP, Serdons K, et al. Validation of Parametric Methods for [(11)C]UCB-J PET Imaging Using Subcortical White Matter as Reference Tissue. *Mol Imaging Biol*. 2020;22(2):444-452.
32. Rossano S, Toyonaga T, Finnema SJ, et al. Assessment of a white matter reference region for (11)C-UCB-J PET quantification. *J Cereb Blood Flow Metab*. 2019:271678X19879230.
33. Bastin C, Bahri MA, Meyer F, et al. In vivo imaging of synaptic loss in Alzheimer's disease with [18F]UCB-H positron emission tomography. *Eur J Nucl Med Mol Imaging*. 2020;47(2):390-402.
34. Gomez-Isla T, Price JL, McKeel DW, Jr., Morris JC, Growdon JH, Hyman BT. Profound loss of layer II entorhinal cortex neurons occurs in very mild Alzheimer's disease. *J Neurosci*. 1996;16:4491-4500.
35. Ghosh S, Brinkman C, Porter R. A quantitative study of the distribution of neurons projecting to the precentral motor cortex in the monkey (M. fascicularis). *J Comp Neurol*.1987;259:424-444.
36. Bates JF, Goldman-Rakic PS. Prefrontal connections of medial motor areas in the rhesus monkey. *J Comp Neurol*. 1993;336:211-228.
37. Padberg J, Cooke DF, Cerkevich CM, Kaas JH, Krubitzer L. Cortical connections of area 2 and posterior parietal area 5 in macaque monkeys. *J Comp Neurol*. 2019;527:718-737.
38. Finnema SJ, Rossano S, Naganawa M, et al. A single-center, open-label positron emission tomography study to evaluate brivaracetam and levetiracetam synaptic vesicle glycoprotein 2A binding in healthy volunteers. *Epilepsia*. 2019;60:958-967.
39. Innis RB, Cunningham VJ, Delforge J, et al. Consensus nomenclature for in vivo imaging of reversibly binding radioligands. *J Cereb Blood Flow Metab*. 2007;27:1533-1539.
40. Yeterian EH, Pandya DN, Tomaiuolo F, Petrides M. The cortical connectivity of the prefrontal cortex in the monkey brain. *Cortex*. 2012;48:58-81.
41. Mooney RD PM. Modulation of Movement by the Cerebellum. In: Purves D AG, Fitzpatrick D, Hall WC, LaMantia AS, White LE, Eds. Neuroscience. 5th ed. Sunderland, MA: Sinauer Associates; 2012. p. 759.
42. Schmahmann JD, Pandya DN. Anatomical investigation of projections to the basis pontis from posterior parietal association cortices in rhesus monkey. *J Comp Neurol*. 1989;289:53-73.
43. Schmahmann JD, Pandya DN. Prefrontal cortex projections to the basilar pons in rhesus monkey: implications for the cerebellar contribution to higher function. *Neurosci Lett*. 1995;199:175-178.
44. Loughlin SE, Foote SL, Grzanna R. Efferent projections of nucleus locus coeruleus: morphologic subpopulations have different efferent targets. *Neuroscience*. 1986;18:307-319.

SUPPORTING INFORMATION

Additional supporting information may be found online in the Supporting Information section at the end of the article.

How to cite this article: Mecca AP, Chen M-K, O'Dell RS, et al. In vivo measurement of widespread synaptic loss in Alzheimer's disease with SV2A PET. *Alzheimer's Dement*. 2020;16:974–982. https://doi.org/10.1002/alz.12097